Interpocket Pairing and Gap Symmetry in Fe-Based Superconductors with Only Electron Pockets

M. Khodas[1] and A. V. Chubukov[2]

[1]*Department of Physics and Astronomy, University of Iowa, Iowa City, Iowa 52242, USA*
[2]*Department of Physics, University of Wisconsin, Madison, Wisconsin 53706, USA*

We analyze the pairing symmetry in Fe-based superconductors $A\mathrm{Fe_2Se_2}$ (A = K, Rb, Cs) which contain only electron pockets. We argue that the pairing condensate in such systems contains not only intrapocket component but also interpocket component, made of fermions belonging to different electron pockets. We analyze the interplay between intrapocket and interpocket pairing, depending on the ellipticity of electron pockets and the strength of their hybridization. We show that with increasing hybridization, the system undergoes a transition from a d-wave state to an s^{+-} state, in which the gap changes sign between hybridized pockets. This s^{+-} state has the full gap and at the same time supports spin resonance, in agreement with the data. Near the boundary between d and s^{+-} states, we found a long-sought $s + id$ state which breaks time-reversal symmetry.

PACS numbers: 74.70.Xa, 74.20.Mn, 74.25.Dw

Introduction.—High-temperature superconductivity in Fe-based superconductors (FeSCs) is at the top of the list of the most relevant issues for the physics community [1–4]. Superconductivity in weakly or moderately doped FeSCs is generally believed to be the consequence of the complex geometry of the Fermi surface (FS), which consists of hole and electron pockets located in separate regions of the Brillouin zone. The prevailing scenario is that the gap has an s-wave symmetry, changes sign between hole and electron pockets [5,6], and may even have accidental nodes [1,7].

This scenario has been challenged recently by the observation of high-temperature superconductivity [8,9] in $A_x\mathrm{Fe_{2-y}Se_2}$ ($A\mathrm{Fe_2Se_2}$) with A = K, Rb, Cs, which have only electron pockets, according to photoemission [10]. Several groups argued [11–14] that interaction between electron pockets in $A\mathrm{Fe_2Se_2}$ plays the same role as intrapocket hole-electron interaction in weakly doped FeSCs, and the gap must change sign between two electron pockets. Such a "plus-minus" gap has no nodes, but it is antisymmetric with respect to the interchange of X and Y directions (along which the two pockets are located), and hence has d-wave symmetry. A no-nodal d-wave gap is, however, rather fragile and was argued [15] to acquire symmetry-related nodes once one includes the hybridization between the electron pockets due to an additional hopping via a chalcogen (Se). The data on $A\mathrm{Fe_2Se_2}$, however, show that the gap has no nodes [16–18], which led other groups to argue [19–21] that the gap in $A\mathrm{Fe_2Se_2}$ must be a sign-preserving s wave. Such gap, however, is also problematic as it is inconsistent with recent observation of the spin resonance below T_c in $\mathrm{Rb_xFe_{2-y}Se_2}$ (Ref. [22]).

In this Letter, we show that a nodeless superconductivity, consistent with the spin resonance, in fact appears quite naturally in a situation when only electron pockets are

present. We argue that complete theory of superconductivity in such geometry should include on equal footing a pairing condensate made out of fermions on the same pocket (intrapocket pairing) and a pairing condensate made out of fermions on different pockets (interpocket pairing). Interpocket pairing has been discussed in the early days of Fe pnictides regarding a possible spin-triplet, even-parity pairing in weakly doped FeSCs [23,24] and in the context of pairing in orbital representation [25], but was not considered in previous works on the pairing in FeSCs with only electron pockets [26]. For $A\mathrm{Fe_2Se_2}$, interpocket pairing is particularly important because both hybridization and ellipticity are small [15]. We show that the interplay between intra- and interpocket pairing leads to a competition between d-wave and s-wave states. We find three phases merging at the tetracritical point—an s wave, an $s + id$ state which breaks time-reversal symmetry, and a d-wave state (Fig. 1). In s-wave and $s + id$ states, all states are gapped. In a d-wave state, there are vertical loop nodes centered $k_z = \pi/2$. In some range of parameters, loops collapse and a d-wave state also becomes nodeless (d' phase in Fig. 1). The s wave is of plus-minus type—the gaps on hybridized FSs have opposite signs. Such a state has been earlier proposed phenomenologically by Mazin [15]. Our study provides the microscopic mechanism of such s^{+-} superconductivity.

The model.—We consider the low-energy physics of FeSCs with only electron pockets within a two-dimensional model of interacting fermions near $(0, \pi)$ and $(\pi, 0)$. The hopping via a pnictogen or chalcogen hybridizes the two electron pockets and also gives rise to additional 4-fermion interactions with excess momentum $Q = (\pi, \pi)$ taken by pnictogen or chalcogen. The hybridization in $A\mathrm{Fe_2Se_2}$ actually involves momentum (π, π, π) because of body-centered tetragonal structure of these
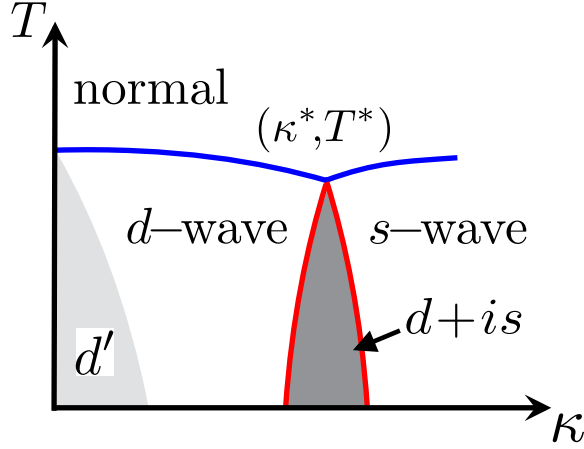
FIG. 1 (color online). The phase diagram in (κ, T) plane for Fe-based superconductors with only electron pockets (κ is the ratio of the hybridization and the degree of ellipticity of the electron pockets). The $s + id$ phase with broken time-reversal symmetry is shown by the dark (gray) shaded area. The two neighboring superconducting phases at $\kappa < (>)\kappa^*$ have $d(s)$-wave symmetry, respectively. In the d' region the excitation spectrum is fully gapped even though the symmetry is d wave.

materials, i.e., hybridized fermions belong to different planes separated by $k_z = \pi$ [15,27]. To simplify the presentation, we first consider hybridization for a simple tetragonal structure, for which hybridized fermions have the same k_z and then extend the analysis to body-centered tetragonal structure.

Let $c_{\boldsymbol{k}}^\dagger$ be a creation operator for electrons at $(0, \pi)$, and $f_{\boldsymbol{k}}^\dagger = c_{\boldsymbol{k}+\boldsymbol{Q}}^\dagger$ is a creation operator of electrons at $(\pi, 0)$. The quadratic part of the Hamiltonian $H = H_2 + H_{\text{int}}$ is

$$H_2 = \sum_{\boldsymbol{k}} \epsilon_{\boldsymbol{k}}^c c_{\boldsymbol{k}}^\dagger c_{\boldsymbol{k}} + \sum_{\boldsymbol{k}} \epsilon_{\boldsymbol{k}}^f f_{\boldsymbol{k}}^\dagger f_{\boldsymbol{k}} + \sum_{\boldsymbol{k}} \lambda[c_{\boldsymbol{k}}^\dagger f_{\boldsymbol{k}} + f_{\boldsymbol{k}}^\dagger c_{\boldsymbol{k}}], \quad (1)$$

where the first two terms describe fermion dispersion, and the last term describes the hybridization. The two elliptical FSs are defined by $\epsilon_{\boldsymbol{k}}^{c(f)} = \epsilon_F$. We approximate fermion excitations near these FSs by $\epsilon_{\boldsymbol{k}}^c = v_F(\phi)[k - k_F(\phi)]$, $\epsilon_{\boldsymbol{k}}^f = v_F(\phi + \pi/2)[k - k_F(\phi + \pi/2)]$, where ϕ is the angle along each of the FSs counted from the x-axis. By virtue of tetragonal symmetry, $v_F(\phi) = v_F(1 + a\cos 2\phi)$ and $k_F(\phi) = k_F(1 + b\cos 2\phi)$. The anisotropy of the Fermi velocity does not play a major role in our analysis, but the eccentricity of the FS (the parameter b) is overly relevant. Both b and $\lambda/(v_F k_F)$ are small for $A\text{Fe}_2\text{Se}_2$ (Ref. [15]), but their ratio $\kappa = \lambda/(v_F k_F |b|)$ can be arbitrary. We set λ to be constant. In general, λ depends on ϕ because of (i) off-plane positioning of Se atoms with respect to Fe atoms, and (ii) orbital structure of hopping integrals between Fe and Se. We verified that the dependence coming from (i) is irrelevant for our analysis, while the dependence from (ii) changes numbers but does not modify our phase diagram, Fig. 1.

The interaction Hamiltonian involves direct, momentum-conserving, 4-fermion interactions, and interactions with excess momentum $\boldsymbol{Q}$. There are four direct interactions allowed by symmetry,

$$H_1 = \frac{u_1}{2} \int d\boldsymbol{x}(c_\sigma^\dagger f_{\sigma'}^\dagger f_{\sigma'} c_\sigma + f_\sigma^\dagger c_{\sigma'}^\dagger c_{\sigma'} f_\sigma)$$

$$H_2 = \frac{u_2}{2} \int d\boldsymbol{x}(c_\sigma^\dagger f_{\sigma'}^\dagger c_{\sigma'} f_\sigma + f_\sigma^\dagger c_{\sigma'}^\dagger f_{\sigma'} c_\sigma)$$

$$H_3 = \frac{u_3}{2} \int d\boldsymbol{x}(c_\sigma^\dagger c_{\sigma'}^\dagger f_{\sigma'} f_\sigma + f_\sigma^\dagger f_{\sigma'}^\dagger c_{\sigma'} c_\sigma)$$

$$H_4 = \frac{u_4}{2} \int d\boldsymbol{x}(c_\sigma^\dagger c_{\sigma'}^\dagger c_{\sigma'} c_\sigma + f_\sigma^\dagger f_{\sigma'}^\dagger f_{\sigma'} f_\sigma). \quad (2)$$

H_1 and H_2 are interband density-density and exchange interactions, H_4 is the intraband density-density interaction, and H_3 describes the umklapp pair-hopping processes. For circular pockets, the couplings u_i are related as there are only three combinations invariant under O(2) rotational symmetry in (c, f) space and SU(2) spin symmetry—n^2, $\boldsymbol{S}^2$, and $\tilde{n}^2$, where $n = c_\alpha^\dagger c_\alpha + f_\alpha^\dagger f_\alpha$ is the total charge density, $\boldsymbol{S} = (1/2)(c_\alpha^\dagger c_\beta + f_\alpha^\dagger f_\beta)\sigma_{\alpha\beta}$ is the total spin, and $\tilde{n} = c_\alpha^\dagger f_\alpha - f_\alpha^\dagger c_\alpha$. Hence $H = Un^2/2 + J'\tilde{n}^2/2 + 2J\boldsymbol{S}^2$, and the interactions u_i are $u_1 = U - J$, $u_2 = -2J - J'$, $u_3 = J'$, $u_4 = U - 3J$. Then $-u = u_4 - u_3 = u_1 + u_2 = U - 3J - J'$. For weak ellipticity, $u_1 + u_2$ and $u_4 - u_3$ do not have to be identical, but remain close and we will keep them equal for simplicity. We will need u to be positive for superconductivity. This is the case when Hund interaction is the dominant one. If u is negative, the system likely develops a magnetic order instead of superconductivity. The interaction with excess momentum $\boldsymbol{Q}$ is

$$H_{\boldsymbol{Q}} = w_1 \int d\boldsymbol{x}(c_\sigma^\dagger f_\sigma + f_\sigma^\dagger c_\sigma)(c_{\sigma'}^\dagger c_{\sigma'} + f_{\sigma'}^\dagger f_{\sigma'}). \quad (3)$$

Other interactions with $\boldsymbol{Q}$ vanish without time-reversal symmetry breaking.

The quadratic Hamiltonian can be diagonalized by unitary transformation to new operators $a_{\boldsymbol{k}} = c_{\boldsymbol{k}}\cos\theta_{\boldsymbol{k}} + f_{\boldsymbol{k}}\sin\theta_{\boldsymbol{k}}$, $b_{\boldsymbol{k}} = -c_{\boldsymbol{k}}\sin\theta_{\boldsymbol{k}} + f_{\boldsymbol{k}}\cos\theta_{\boldsymbol{k}}$ with $\sin 2\theta_{\boldsymbol{k}} = \lambda/\sqrt{\lambda^2 + (\epsilon_{\boldsymbol{k}}^c - \epsilon_{\boldsymbol{k}}^f)^2/4}$, $\cos 2\theta_{\boldsymbol{k}} = (\epsilon_{\boldsymbol{k}}^c - \epsilon_{\boldsymbol{k}}^f)/(2\sqrt{\lambda^2 + (\epsilon_{\boldsymbol{k}}^c - \epsilon_{\boldsymbol{k}}^f)^2/4})$. In terms of new operators,

$$H_2 = \sum_{\boldsymbol{k}} E_{\boldsymbol{k}}^a a_{\boldsymbol{k}}^\dagger a_{\boldsymbol{k}} + \sum_{\boldsymbol{k}} E_{\boldsymbol{k}}^b b_{\boldsymbol{k}}^\dagger b_{\boldsymbol{k}}, \quad (4)$$

with

$$E_{\boldsymbol{k}}^{a,b} = \frac{1}{2}(\epsilon_{\boldsymbol{k}}^c + \epsilon_{\boldsymbol{k}}^f) \pm [\lambda^2 + (\epsilon_{\boldsymbol{k}}^c - \epsilon_{\boldsymbol{k}}^f)^2/4]^{1/2}. \quad (5)$$

In our notations, $(\epsilon_{\boldsymbol{k}}^c + \epsilon_{\boldsymbol{k}}^f)/2 \approx \epsilon_F + v_F(k - k_F) = \epsilon_F + \xi$, and $(\epsilon_{\boldsymbol{k}}^c - \epsilon_{\boldsymbol{k}}^f)/2 \approx v_F k_F b\cos 2\phi$, such that $E_{\boldsymbol{k}}^{a,b} - \epsilon_F = \xi \pm \lambda(1 + \cos^2 2\phi/\kappa^2)^{1/2}$, $\cos^2 2\theta = \cos^2 2\phi/(\kappa^2 + \cos^2 2\phi)$, and $\sin^2 2\theta = \kappa^2/(\kappa^2 + \cos^2 2\phi)$.

The interplay between intrapocket and interpocket pairing can be understood by considering the limits of small and large κ (Fig. 2). At $\kappa \to 0$ the hybridization vanishes, and c and f are primary operators. For elliptical pockets, intrapocket pairing susceptibility is larger than interpocket, and when $u_3 > u_4$, the system develops a conventional pairing instability with $\Delta_c = \langle c_\uparrow^\dagger c_\downarrow^\dagger \rangle$ and $\Delta_f = \langle f_\uparrow^\dagger f_\downarrow^\dagger \rangle$ and $\Delta_f = -\Delta_c$ [Fig. 2(a)]. This solution is antisymmetric with respect to $c \leftrightarrow f$ and hence is d wave. In the opposite limit of large κ, a and b are primary fermion operators, and the FSs of a and b fermions are well separated in the momentum space [Fig. 2(b)]. The leading pairing instability is again a conventional intrapocket one, and the gaps $\Delta_a = \langle a_\uparrow^\dagger a_\downarrow^\dagger \rangle$ and $\Delta_b = \langle b_\uparrow^\dagger b_\downarrow^\dagger \rangle$ obey $\Delta_a = -\Delta_b$. This gap, however, is a sign-changing s wave rather than a d wave. To see this, we note that at large κ, $a_\uparrow^\dagger a_\downarrow^\dagger - b_\uparrow^\dagger b_\downarrow^\dagger = c_\uparrow^\dagger f_\downarrow^\dagger + f_\uparrow^\dagger c_\downarrow^\dagger$, i.e., the solution $\Delta_a = -\Delta_b$ corresponds to nonzero $\langle c_\uparrow^\dagger f_\downarrow^\dagger + f_\uparrow^\dagger c_\downarrow^\dagger \rangle$. The latter combination is symmetric with respect to $c \leftrightarrow f$ and hence is an s wave, but it also shows that in terms of c and f fermions, we now have interpocket pairing. What happened with the d-wave solution? At large κ, we have $c_\uparrow^\dagger c_\downarrow^\dagger - f_\uparrow^\dagger f_\downarrow^\dagger = -(a_\uparrow^\dagger b_\downarrow^\dagger + b_\uparrow^\dagger a_\downarrow^\dagger)$. Hence, in terms of a and b operators, d-wave pairing now becomes interpocket pairing. We see therefore that intrapocket pairing in terms of one set of fermions corresponds to interpocket pairing in terms of the other set. To describe the transformation from d to s-wave symmetry, we then have to include the two pairings on equal footing.

It is natural to analyze the pairing in terms of a and b fermions because the Hamiltonian, Eq. (1), is then quadratic at all values of κ. We introduce intra- and interband pair creation operators,

$$J_\pm^\dagger = \tfrac{1}{2}(a^\dagger a^\dagger \pm b^\dagger b^\dagger), \qquad \tilde{J}_\pm^\dagger = \tfrac{1}{2}(a^\dagger b^\dagger \pm b^\dagger a^\dagger). \quad (6)$$

The combinations $J_+^\dagger$ and $\tilde{J}_-^\dagger$ describe an ordinary, "plus-plus" s-wave pairing and spin-triplet, even parity interband pairing, respectively (the triplet channel is identical to the one considered in [23]). In our case, these two pairing channels are strongly repulsive, and we can safely omit
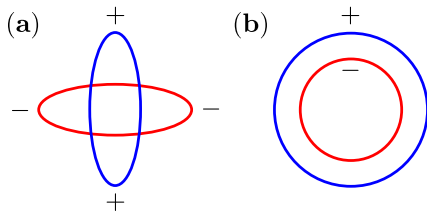

FIG. 2 (color online).   The structure of superconducting gap at small and large κ. At the smallest κ, panel (a), the gap has a different sign on the original FS pockets and is d wave because it is antisymmetric with respect to rotation by 90°. At large κ, panel (b), the gap again changes sign, but now between hybridized FS pockets. This gap is symmetric with respect to 90° rotation and is an s wave.

them. The linear combinations of the other two components $J_-^\dagger$ and $\tilde{J}_+^\dagger$ describe s-wave pair creation operators

$$\tfrac{1}{2}(c_\sigma^\dagger f_{\sigma'}^\dagger + f_\sigma^\dagger c_{\sigma'}^\dagger) = [\cos 2\theta \tilde{J}_+^\dagger + \sin 2\theta J_-^\dagger]_{\sigma\sigma'} \quad (7)$$

and d-wave pair creation operators

$$\tfrac{1}{2}(c_\sigma^\dagger c_{\sigma'}^\dagger - f_\sigma^\dagger f_{\sigma'}^\dagger) = [\cos 2\theta J_-^\dagger - \sin 2\theta \tilde{J}_+^\dagger]_{\sigma\sigma'}, \quad (8)$$

The interaction, Eq. (2), can then be decomposed into an s-wave and d-wave channel, $H_{\text{int}} = H_s + H_d$ with

$$H_s = -2u[s'J_-^\dagger + c'\tilde{J}_+^\dagger]_{\sigma\sigma'}[sJ_- + c\tilde{J}_+]_{\sigma'\sigma}, \quad (9)$$

$$H_d = -2u[c'J_-^\dagger - s'\tilde{J}_+^\dagger]_{\sigma\sigma'}[cJ_- - s\tilde{J}_+]_{\sigma'\sigma}, \quad (10)$$

where $c \equiv \cos 2\theta$, $c' \equiv \cos 2\theta'$, $s \equiv \sin 2\theta$, $s' \equiv \sin 2\theta'$. We emphasize that the intra- and interband pairings enter Eqs. (9) and (10) on equal footing. The interaction H_Q couples these two channels with plus-plus s-wave channel and spin-triplet channels which we already neglected, and does not play a role in our analysis.

Ginzburg-Landau functional.—To map a phase diagram in (κ, T) plane, we derive the Ginzburg-Landau functional (GLF). We introduce order parameters Δ_s and Δ_d to decouple the interaction in two Cooper channels using the Hubbard-Stratonovitch identity, integrate over fermion fields, and expand the effective action in powers of Δ_s and Δ_d. Carrying out the calculations (see Supplemental Material [28] for details), we obtain

$$F_{\text{GL}} = A_s|\Delta_s|^2 + A_d|\Delta_d|^2 + \frac{B_s}{2}|\Delta_s|^4 + \frac{B_d}{2}|\Delta_d|^4$$
$$+ C|\Delta_s|^2|\Delta_d|^2 + \frac{E}{2}((\Delta_s\Delta_d^*)^2 + (\Delta_s^*\Delta_d)^2). \quad (11)$$

The transition to either s-wave or d-wave state is determined by $A_s = 0$ or $A_d = 0$, whichever comes first. The lines $A_s = 0$ and $A_d = 0$ cross at some critical κ^*, at which $T_c = T_c^*$. For $\lambda \gg T_c^*$ (the case of AFe$_2$Se$_2$, Ref. [15]), we obtain $\kappa^* = 1/\sqrt{3}$ [in the other limit $\lambda \ll T_c^*$ $\kappa^* = 1/\sqrt{2}$ (see Supplemental Material [28] for derivation)]. Near the critical κ, the first instability occurs at $T_{c,s} = T_c^*[1 + \alpha(\kappa - \kappa^*)]$ for $\kappa > \kappa^*$ and at $T_{c,d} = T_c^*[1 + \alpha(\kappa^* - \kappa)]$ for $\kappa < \kappa^*$, where $\alpha = 3\sqrt{3}/(2uN_F)$ (see Fig. 1).

The type of the transition from a d-wave order at $\kappa < \kappa^*$ to an s-wave order at $\kappa > \kappa^*$ is determined by the interplay between fourth-order terms in Eq. (11). The transition can be either first-order or continuous, via an intermediate phase where both orders are present. At $T = T_c^*$ we obtained $B_s = B_d = B = \frac{5}{8}I_0$, $C = \frac{3}{8}I_0$, and $E = C/2$, where $I_0 = 7\zeta(3)/8\pi^2(T_c^*)^2$. We see that $E > 0$ and $B + E > C$. An elementary analysis then shows that the transition from d to s involves an intermediate phase in which the two orders mix with relative phase $\pm\pi/2$. This is long-sought $s \pm id$ state [29,30]. The system chooses either $s + id$ or $s - id$ state and by doing this breaks time-reversal symmetry. An $s + id$ state contains orbital currents and should be
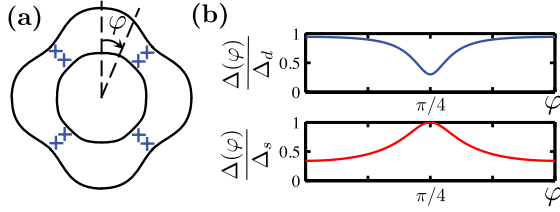
FIG. 3 (color online).   (a) Location of the nodal points in the
d-wave phase (crosses). Upon approaching the boundary of d'
phase in Fig. 1, nodal points come closer and eventually col-
lapse, leading to a nodeless d-wave state. (b) The modulation of
the gap magnitude along the FSs for d-wave and s-wave states.

detectable in, e.g., neutron scattering [31] and Josephson
junction experiments [32]. The boundaries of this intermedi-
ate phase are set by $T_{s+id} = T_c^*(1 - \beta|\kappa - \kappa^*|)$, where $\beta = 6\sqrt{3}/(uN_F)$. We emphasize again that both the transition
from s to d and the existence of the intermediate phase are
due to the competition between intrapocket and interpocket
pairing.

Fermion excitations.—In the s-wave state and in the
intermediate $s \pm id$ state, excitations are fully gapped. In
the d-wave state, the excitation spectrum is given (see
Supplemental Material [28]):

$$\omega_\pm^2 = |\Delta_d|^2\cos^2 2\theta + \left(\sqrt{\xi^2 + |\Delta_d|^2\sin^2 2\theta} \pm \frac{\lambda}{\sin 2\theta}\right)^2,$$
(12)

where, we remind, $\xi \approx v_F(k - k_F)$. The dispersion ω_-
has nodes along the diagonal directions where $\cos 2\theta = 0$,
as it should be for a d-wave superconductor. However, the
nodal points are located in between a and b FSs, as shown
in Fig. 3(a). This is another consequence of interpocket
pairing. We plot the dispersions in s and d-wave states in
Fig. 3(b). We furthermore see from (12) that nodes in the
d-wave state exist only if $|\Delta_d| < \lambda$; otherwise, the second
term in the right-hand side of (12) does not vanish even
when $\xi = 0$. The condition $|\Delta_d| = \lambda$ then sets the bound-
ary of the nodeless d-wave state (d' state on Fig. 1).

Application to $A\mathrm{Fe}_2\mathrm{Se}_2$.—The hybridization of electron
pockets in $A\mathrm{Fe}_2\mathrm{Se}_2$ is more involved because of the body-
centered tetragonal structure of these materials [8]. The
two hybridized electron FSs differ by $k_z = \pi$ and are
rotated by $\pi/2$ (see Figs. 4(a)–4(c) and Refs. [15,27]).
For $k_z = 0$ and $k_z = \pi$, the FS in the folded zone consists
of coaligned ellipses [Figs. 4(d)–4(f)], the pair near (π, π)
at $k_z = 0$ is identical to the one near $(-\pi, \pi)$ at $k_z = \pi$.
At $k_z = \pm\pi/2$, the pockets are C_4 symmetric already
before hybridization, and the hybridization leads to iden-
tical pairs at (π, π) and $(-\pi, \pi)$. s-wave and d-wave gaps
differ in whether the gap on the larger ellipsis retains
sign or changes sign between $k_z = 0$ $k_z = \pi$ [Figs. 4(g)
and 4(h)]. Near $k_z = \pi/2$, the hybridization instantly fa-
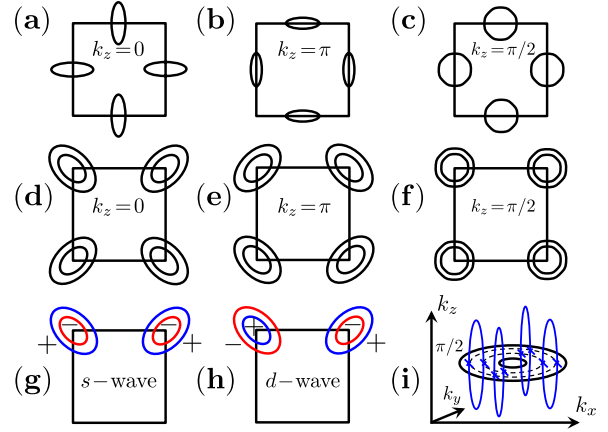vors s wave, if we approximate C_4-symmetric pockets as

FIG. 4 (color online).   The structure of electronic states and the
superconducting gap in $A\mathrm{Fe}_2\mathrm{Se}_2$ which have body-centered
tetragonal structure. Panels (a)–(c): electron pockets in the
unfolded Brillouin zone for different k_z. Panels (d)–(f): same
in the folded zone. The two ellipses at each corner remain coaxial
and rotate by 90° between $k_z = 0$ and $k_z = \pi$. Panels (g)–(h):
s-wave and d-wave gap structure near $k_z = 0$ and $k_z = \pi$. Panel
i: the location of the nodes at $k_z \approx \pi/2$. The nodal points form
vertical loops (only two are shown for clarity). If hybridized
FSs at $\pi/2$ are two circles, the crosses extend and form lines in
(k_x, k_y) plane (dashed lines in the figure).

circles, but overall which of the two states is realized
depends on κ averaged along k_z and on the strength of k_z
dependence of the interaction u. Note that in a d-wave
state, nodes exist near $k_z = \pi/2$, but not near $k_z = 0$ and
$k_z = \pi$, where the two FSs in the same corner in the folded
zone are separated—they are coaxial ellipses of different
sizes, and hybridization only causes minor variations of
originally angle-independent gap (this behavior is the same
as in d' region in Fig. 1). Because of this, the nodes in the
d-wave state form vertical loops centered at $k_z = \pi/2$
[Fig. 4(i)]. Vertical loop nodes have been earlier suggested
on phenomenological grounds [33,34] but have not been
obtained microscopically earlier.

To conclude, in this Letter we argued that the pairing in
Fe-based superconductors with only electron pockets must
necessarily include inter-band condensate made of fermions
belonging to different pockets. We demonstrated that the
interplay between intrapocket and interpocket pairing leads
to a transition from d-wave pairing at a small degree of
hybridization to an s^{+-}-wave pairing at larger hybridiza-
tion. In between, there is an intermediate $s \pm id$ state with
broken time-reversal symmetry. Fermionic excitations in
s^{+-} and $s + id$ states are fully gapped, yet in both states
there is the spin resonance below T_c [15,35,36]. The absence
of the nodes and the existence of the spin resonance are
consistent with the data on $A\mathrm{Fe}_2\mathrm{Se}_2$ [8,22], which makes
s^{+-} state and, potentially, $s + id$ state the likely candidates.

[1] A. F. Kemper, T. A. Maier, S. Graser, H.-P. Cheng, P. J. Hirschfeld, and D. J. Scalapino, New J. Phys. **12**, 073030 (2010).

[2] P. J. Hirschfeld, M. M. Korshunov, and I. I. Mazin, Rep. Prog. Phys. **74**, 124508 (2011).

[3] A. V. Chubukov, Annu. Rev. Condens. Matter Phys. **3**, 57 (2012).

[4] H. H. Wen and S. Li, Annu. Rev. Condens. Matter Phys. **2**, 121 (2011).

[5] I. I. Mazin, D. J. Singh, M. D. Johannes, and M. H. Du, Phys. Rev. Lett. **101**, 057003 (2008).

[6] K. Kuroki, S. Onari, R. Arita, H. Usui, Y. Tanaka, H. Kontani, and H. Aoki, Phys. Rev. Lett. **101**, 087004 (2008).

[7] A. V. Chubukov, M. G. Vavilov, and A. B. Vorontsov, Phys. Rev. B **80**, 140515(R) (2009).

[8] J. Guo, S. Jin, G. Wang, S. Wang, K. Zhu, T. Zhou, M. He, and X. Chen, Phys. Rev. B **82**, 180520(R) (2010).

[9] See Y. Liu, Z. C. Li, W. P. Liu, G. Friemel, D. S. Inosov, R. E. Dinnebier, Z. J. Li, and C. T. Lin, arXiv:1201.0902 and references therein.

[10] T. Qian, X.-P. Wang, W.-C. Jin, P. Zhang, P. Richard, G. Xu, X. Dai, Z. Fang, J.-G. Guo, X.-L. Chen, and H. Ding, Phys. Rev. Lett. **106**, 187001 (2011).

[11] T. A. Maier, S. Graser, P. J. Hirschfeld, and D. J. Scalapino, Phys. Rev. B **83**, 100515(R) (2011).

[12] T. Das and A. V. Balatsky, Phys. Rev. B **84**, 014521 (2011); **84**, 115117 (2011).

[13] F. Wang, F. Yang, M. Gao, Z.-Y. Lu, T. Xiang, and D.-H. Lee, Europhys. Lett. **93**, 57003 (2011).

[14] S. Maiti, M. M. Korshunov, T. A. Maier, P. J. Hirschfeld, and A. V. Chubukov, Phys. Rev. B **84**, 224505 (2011); Phys. Rev. Lett. **107**, 147002 (2011).

[15] I. I. Mazin, Phys. Rev. B **84**, 024529 (2011).

[16] Y. Zhang, L. X. Yang, M. Xu, Z. R. Ye, F. Chen, C. He, J. Jiang, B. P. Xie, J. J. Ying, X. F. Wang, X. H. Chen, J. P. Hu, and D. L. Feng, Nat. Mater. **10**, 273 (2011).

[17] D. Mou, S. Liu, X. Jia, J. He, Y. Peng, L. Zhao, Li Yu, G. Liu, S. He, X. Dong, J. Zhang, H. Wang, C. Dong, M. Fang, X. Wang, Q. Peng, Z. Wang, S. Zhang, F. Yang, Z. Xu, C. Chen, and X. J. Zhou, Phys. Rev. Lett. **106**, 107001 (2011).

[18] X.-P. Wang, T. Qian, P. Richard, P. Zhang, J. Dong, H.-D. Wang, C.-H. Dong, M.-H. Fang, and H. Ding, Europhys. Lett. **93**, 57001 (2011).

[19] R. Yu, P. Goswami, Q. Si, P. Nikolic, and J.-X. Zhu, Phys. Rev. B **84**, 094451 (2011).

[20] C. Fang, Y.-L. Wu, R. Thomale, B. A. Bernevig, and J. Hu, Phys. Rev. X **1**, 011009 (2011).

[21] T. Saito, S. Onari, and H. Kontani, Phys. Rev. B **83**, 140512(R) (2011).

[22] J. T. Park, G. Friemel, Y. Li, J.-H. Kim, V. Tsurkan, J. Deisenhofer, H.-A. Krug von Nidda, A. Loidl, A. Ivanov, B. Keimer, and D. S. Inosov, Phys. Rev. Lett. **107**, 177005 (2011).

[23] X. Dai, Z. Fang, Y. Zhou, and F.-C Zhang, Phys. Rev. Lett. **101**, 057008 (2008).

[24] I. I. Mazin, M. D. Johannes, L. Boeri, K. Koepernik, and D. J. Singh, Phys. Rev. B **78**, 085104 (2008).

[25] A. Moreo, M. Daghofer, A. Nicholson, and E. Dagotto, Phys. Rev. B **80**, 104507 (2009).

[26] Interpocket pairing has been discussed for other systems, most recently for intervalley pairing in graphene: M. Einenkel and K. B. Efetov, Phys. Rev. B **84**, 214508 (2011).

[27] J. T. Park, D. S. Inosov, A. Yaresko, S. Graser, D. L. Sun, Ph. Bourges, Y. Sidis, Yuan Li, J.-H. Kim, D. Haug, A. Ivanov, K. Hradil, A. Schneidewind, P. Link, E. Faulhaber, I. Glavatskyy, C. T. Lin, B. Keimer, and V. Hinkov, Phys. Rev. B **82**, 134503 (2010).

[28] See Supplemental Material at http://link.aps.org/supplemental/10.1103/PhysRevLett.108.247003 for details and derivation.

[29] K. A. Musaelian, J. Betouras, A. V. Chubukov, and R. Joynt, Phys. Rev. B **53**, 3598 (1996); Meng Cheng, Kai Sun, Victor Galitski, and S. Das Sarma, Phys. Rev. B **81**, 024504 (2010).

[30] See C. Platt, R. Thomale, C. Honerkamp, S.-C. Zhang, and W. Hanke, arXiv:1106.5964 for a different scenario for $s + id$ state.

[31] See, e.g., Y. Li, V. Baledent, N. Barisic, P. Bourges, Y. Cho, B. Fauque, Y. Sidis, G. Yu, X. Zhao, and M. Greven, Nature (London) **455**, 372 (2008).

[32] D. Van Harlingen, Rev. Mod. Phys. **67**, 515 (1995).

[33] M. Yamashita, Y. Senshu, T. Shibauchi, S. Kasahara, K. Hashimoto, D. Watanabe, H. Ikeda, T. Terashima, I. Vekhter, A. B. Vorontsov, and Y. Matsuda, Phys. Rev. B **84**, 060507(R) (2011).

[34] I. I. Mazin, T. P. Devereaux, J. G. Analytis, Jiun-Haw Chu, I. R. Fisher, B. Muschler, and R. Hackl, Phys. Rev. B **82**, 180502(R) (2010).

[35] M. M. Korshunov and I. Eremin, Phys. Rev. B **78**, 140509 (R) (2008).

[36] T. A. Maier and D. J. Scalapino, Phys. Rev. B **78**, 020514 (R) (2008).